blood advances

Improving stroke outcomes in hyperglycemic mice by modulating tPA/NMDAR signaling to reduce inflammation and hemorrhages

Florent Lebrun,[1,2] Damien Levard,[1] Eloïse Lemarchand,[1] Mervé Yetim,[1] Jonathane Furon,[1] Fanny Potzeha,[1] Pauline Marie,[1] Flavie Lesept,[3] Manuel Blanc,[3] Benoit Haelewyn,[4,5] Marina Rubio,[1] Annelise Letourneur,[2] Nicolas Violle,[2] Cyrille Orset,[1,5,*] and Denis Vivien[1,5,6,*]

[1]Normandie University, UNICAEN, INSERM UMR-S U1237, Physiopathology and Imaging of Neurological Disorders, GIP Cyceron, Institute Blood and Brain @ Caen-Normandie, Caen, France; [2]STROK@LLIANCE, ETAP-Lab, Caen, France; [3]Lys Therapeutics, HQ: Cyceron, Caen, France; [4]GIP Cyceron, Caen, France; [5]Experimental Stroke Research Platform, Normandie University, CURB, Caen, France; and [6]Department of Clinical Research, Caen-Normandie University Hospital, Caen, France

Key Points

- The gold standard thrombolytic agent tPA worsens inflammation and hemorrhagic transformation risk in a hyperglycemic mouse stroke model.

- Glunomab immunotherapy counters side effects of tPA via NMDAR signaling in hyperglycemic mice after stroke.

The pharmacological intervention for ischemic stroke hinges on intravenous administration of the recombinant tissue-type plasminogen activator (rtPA, Alteplase/Actilyse) either as a standalone treatment or in conjunction with thrombectomy. However, despite its clinical significance, broader use of rtPA is constrained because of the risk of hemorrhagic transformations (HTs). Furthermore, the presence of diabetes or chronic hyperglycemia is associated with an elevated risk of HT subsequent to thrombolysis. This detrimental impact of tPA on the neurovascular unit in patients with hyperglycemia has been ascribed to its capacity to induce endothelial N-methyl-D-aspartate receptor (NMDAR) signaling, contributing to compromised blood-brain barrier integrity and neuroinflammatory processes. In a mouse model of thromboembolic stroke with chronic hyperglycemia, we assessed the effectiveness of rtPA and N-acetylcysteine (NAC) as thrombolytic agents. We also tested the effect of blocking tPA/NMDAR signaling using a monoclonal antibody, Glunomab. Magnetic resonance imaging, speckle contrast imaging, flow cytometry, and behavioral tasks were used to evaluate stroke outcomes. In hyperglycemic animals, treatment with rtPA resulted in lower recanalization rates and increased HTs. Conversely, NAC treatment reduced lesion sizes while mitigating HTs. After a single administration, either in standalone or combined with rtPA-induced thrombolysis, Glunomab reduced brain lesion volumes, HTs, and neuroinflammation after stroke, translating into improved neurological outcomes. Additionally, we demonstrated the therapeutic efficacy of Glunomab in combination with NAC or as a standalone strategy in chronic hyperglycemic animals. Counteracting tPA-dependent endothelial NMDAR signaling limits ischemic damages induced by both endogenous and exogenous tPA, including HTs and inflammatory processes after ischemic stroke in hyperglycemic animals.

Introduction

In ischemic stroke, restoration of vessel patency is crucial to mitigate tissue damage and patient deficits.[1-3] Pharmacological strategies aimed at promoting rapid reperfusion rely on the use of recombinant tissue-type plasminogen activator (rtPA) or tenecteplase, either alone or in combination with thrombectomy.[4-6] Despite their clinical effectiveness, the broader application and advancement of thrombolytic therapies remain subjects of debate because of the risk of hemorrhagic transformations (HTs). Moreover, the rate of arterial recanalization after rtPA administration remains relatively low (<30%), particularly in cases in which occlusive thrombi are rich in platelets.[7-10] Consequently, there exists a pressing clinical need to mitigate the side effects associated with thrombolytics, enhancing their efficacy for a larger proportion of patients.

In addition to its role in vascular fibrinolysis,[11] tPA has been recognized for its impact on neuronal survival[12-14] and its ability to modulate the integrity of the blood-brain barrier (BBB) and inflammation.[15-18] These functions of tPA have been associated with the modulation of N-methyl-D-aspartate receptor (NMDAR) signaling, both in neurons and endothelial cells.[12,13,19-21]

It is accepted that the development of an inflammatory response after an ischemic stroke is associated with more severe outcomes, including higher National Institutes of Health Stroke Scale scores and worse Glasgow Coma Scale scores. This inflammatory response also leads to an increased mortality.[22-24] Recent data have highlighted the potential impact of these mechanisms in hemorrhagic strokes.[25-27] Interestingly, there is growing evidence indicating that both endogenous and exogenous tPA play a role in the inflammatory processes after a stroke.[28-30] For example, tPA-NMDAR mechanisms involving endothelial cells may contribute to the infiltration of immune cells into the brain parenchyma.[28,31,32]

It is recognized that diabetes is a significant vascular comorbidity with clinical implications that leads to lower rates of vessel recanalization and risk of HTs. These adverse effects are attributed to factors such as hyperglycemia, oxidative stress, and inflammation. Diabetes is also associated with diminished functional and cognitive outcomes and an elevated risk of mortality.[33] Preclinical studies in hyperglycemic or diabetic animal models have consistently demonstrated adverse effects, including larger infarct sizes in rodents,[34,35] reduced cerebral blood flow, increased edema, higher incidences of HTs,[36] and more severe cognitive deficits.[37] Moreover, patients with diabetes receiving thrombolytic treatment have an increased susceptibility to HTs.[38,39] The risk of stroke is also significantly elevated, with diabetes increasing this risk by 1.5-fold.[40]

Therefore, here, we examined the potential adverse effects of rtPA in a mouse model of thromboembolic stroke with concomitant chronic hyperglycemia. Our investigation encompassed the assessment of outcomes such as HTs and proinflammatory processes, with a focus on whether these effects could be mitigated by inhibiting tPA-dependent endothelial NMDAR signaling. Additionally, we explored the feasibility of substituting rtPA with the safer thrombolytic agent, N-acetylcysteine (NAC).

Materials and methods

Also see supplemental Materials.

Animals

All procedures adhered to the ethical guidelines of the European Directive (2010/63/EU) and were approved by the ethical committee of the Ministry of Higher Education and Research. The experiments followed the Animal Research: Reporting In Vivo Experiments guidelines and were approved under the reference number 21620.

We conducted experiments using male Swiss mice (6 weeks of age, Janvier Laboratories) (Le Genest-Sainte-Isle, France). Animals were maintained in standard husbandry conditions (temperature: $22 \pm 2°C$; hygrometry: $50\% \pm 20\%$) under light–dark cycle (light from 8:00 to 20:00) with ad libitum access to water and food (except on the days of blood glucose levels assessments for which animals fasted for 5 hours). Enrichment materials were provided with 5 animals per cage. Randomization of mice was performed. Experiments and analyses were carried out blinded. The determination of the number of animals per group was based on previous experiments and a meta-analysis involving >700 animals.[4,41]

Thromboembolic stroke

To induce proximal occlusion of the middle cerebral artery (MCA), we used the in situ thromboembolic stroke model consisting in the injection of thrombin directly into the MCA.[5] Under aseptic conditions, animals were anesthetized with 5% isoflurane and maintained with 2% isoflurane in a 70%:30% mixture of NO_2:O_2. Buprenorphine was injected subcutaneously (0.5 mg/kg) and local anesthesia was performed by instillation of lidocaine in both ears. Rectal temperature was maintained at $37 \pm 0.5°C$ throughout the surgical procedure. Mice were placed in a stereotaxic frame; the MCA was exposed through a small craniotomy and the dura excised. A pulled glass micropipette was introduced into the MCA and 1 μL (1 UI/μL) of purified murine α-thrombin (Stago, Belgium) was injected to induce occlusion (MCAo). The pipette was removed 10 minutes after.

Drugs and treatments

Because an aim of the this study was to investigate the potential impact of hyperglycemia, we decided to use a mouse model of type 1 diabetes induced by repeated injections of low doses of streptozotocin (STZ, see supplemental Materials and methods).[42-44] After stroke, a catheter was inserted into the tail vein to allow intravenous administration of 200 μL of treatments or their vehicle 20 minutes or 4 hours after the injection of thrombin. rtPA (Actilyse, Boehringer Ingelheim) at 10 mg/kg was infused at 10% bolus and 90% perfusion for 40 minutes. For NAC injection, mice received 400 mg/kg of NAC (Sigma-Aldrich) dissolved in phosphate-buffered saline. This dosage was determined through a dose escalation study, consistent with our prior research.[41] In addition, 300 μg of Glunomab were administered as an intravenous bolus before infusion of rtPA or its vehicle. Administration of NAC was performed as an intravenous bolus.

Results

tPA loses its beneficial effects and increases the risk of HTs in hyperglycemic mice

We have previously developed a thromboembolic ischemic stroke model in mice,[5] associated, here, with chronic hyperglycemia as a

diabetes-like comorbidity. STZ-induced hyperglycemia was confirmed in an independent cohort, with blood glucose levels reaching 347.5 ± 135.2 mg/dL 16 days after treatment (compared with 157.3 ± 22.9 mg/dL for the control groups, $P < .05$; supplemental Figure 1B). This increase in glucose levels was followed by a loss of weight in STZ-treated animals (33.2 ± 0.9 g in the STZ group, 38.8 ± 1.5 g in vehicle group, 19 days after the end of STZ treatment, $P < .0001$; supplemental Figure 1B). Twenty-seven days after STZ treatments, there was no longer a statistical difference between the 2 groups in terms of body weight (35.7 ± 1.8 g in the STZ group; 38.0 ± 1.9 g in the vehicle group). Hyperglycemia (supplemental Figures 1B, 2, 3A, 5A, and 6A) was maintained until day 14, on which stroke was induced (supplemental Figure 1B), and for the rest of the experiments. We then measured lesion volumes, recanalization, reperfusion rates, and HTs using in vivo magnetic resonance imaging (MRI) and speckle contrast imaging, at day 1 after stroke (Figure 1A). A grip-test task was used to evaluate functional outcomes. No mortality was observed in any group of animals (supplemental Figure 1B). Hyperglycemic animals (STZ) displayed bigger ischemic lesion volumes (23.38 ± 7.3 mm^3 in the control [Ctrl] group vs 36.00 ± 10.8 mm^3 in the STZ group, n = 12-13, $P = .0017$; Figure 1B-C). Early intravenous administration of rtPA (10 mg/kg, 20 minutes after MCAo) diminished the lesion size by 44.9% in the non-hyperglycemic animals, whereas it had no effect in the hyperglycemic animals (23.38 ± 7.3 mm^3 in Ctrl vs 12.88 ± 5.9 mm^3 in Ctrl-rtPA, $P < .01$; and 36 ± 10.8 mm^3 in STZ group vs 39.58 ± 7.6 mm^3 in STZ-rtPA, $P = .7$, n = 13). Hyperglycemic animals displayed a similar rtPA-mediated reperfusion of the injured tissues at 40 minutes after treatment than that in nonhyperglycemic animals (+$15.91\% \pm 4.8\%$ in Ctrl-rtPA vs +$14.06\% \pm 6.2\%$ in STZ-rtPA, n = 12-13, $P = .87$; supplemental Figure 1C). However, 24 hours after MCAo (Figure 1D; supplemental Figure 1A) angiographic scores revealed that nonhyperglycemic and hyperglycemic animals responded to rtPA treatment in terms of recanalization (38% of complete recanalization in Ctrl groups vs 83% of complete recanalization in Ctrl-rtPA group, and 17% of complete recanalization in STZ groups vs 58% in STZ-rtPA groups; n = 12-13). In parallel, hyperglycemic animals treated with rtPA displayed a high level of HTs assessed by using T2*-weighted MRI (Figure 1E; supplemental Figure 1A). This phenomenon was not observed in nonhyperglycemic animals (38% with signs of HT, petechial, and parenchymal hemorrhage, in Ctrl-rtPA, n = 13 vs 67% with signs of HT in STZ-rtPA group, n = 12). A parallel behavior task, the grip test, was performed on days 1, 3, and 7 after stroke onset (Figure 1F-G). Furthermore, mice in all groups displayed sensorimotor deficit at day 1 (day 1 vs day 0, $ P < .05$ in all groups). The strength ratio of left/right paws was significantly improved in the Ctrl-rtPA group (0.92 ± 0.07, n = 12) compared with that of the STZ-rtPA group (0.81 ± 0.09, n = 12). Animals treated with rtPA showed less deficit because of the stroke if they did not present comorbidity. At day 3, the strength ratio of left/right paws remained significantly different from that at baseline in the STZ group, whereas the Ctrl group demonstrated a more pronounced recovery (Figure 1F). Concerning the strength of both paws compared with that at baseline, tPA allowed a better outcome in nonhyperglycemic mice on days 1 and 7 but not in hyperglycemic mice. For this parameter, we also observed a better improvement in non-hyperglycemic mice than in hyperglycemic mice (on day 1: $88.1\% \pm 5.0\%$ in Ctrl-rtPA, n = 12 vs $77.5\% \pm 9.0\%$ in STZ-rtPA

group, n = 12; on ay 3: $91.1\% \pm 5.3\%$ in Ctrl-rtPA vs $84.4\% \pm 10.2\%$ in STZ-rtPA group; on D7: $95.4\% \pm 4.4\%$ in Ctrl-rtPA vs $88.8\% \pm 11.8\%$ in STZ-rtPA group; Figure 1G).

It is well-known in clinical practice that rtPA-induced thrombolysis is beneficial within a limited therapeutic window (4.5 hours alone, and 6-12 hours when combined with thrombectomy).[45] We tested rtPA at 2 times after stroke, within the therapeutic window (ie, 20 minutes) and outside of this window (ie, 4 hours),[4,5,41] to evaluate whether the rate of HTs was also increased with time to treatment in hyperglycemic mice. Our data (Figure 2) confirmed previous results (Figure 1), showing that both early and late rtPA treatments (Figure 2A) led to higher levels of HTs in hyperglycemic animals, without providing brain protection, despite similar recanalization rates compared with those of the STZ group (80% of parenchymal and petechial hemorrhages for early and late rtPA-treated animals, n = 5 compared with 20% in nontreated animals, n = 10; Figure 2B-E). These data demonstrate that chronic hyperglycemia induces a partial resistance to the rtPA treatment and increases the risk of HT, without exacerbating these risks when thrombolysis is delayed.

NAC induces recanalization after acute thrombosis in hyperglycemic animals without the risk of HTs

In a previous work, we demonstrated that intravenous NAC administration, by targeting von Willebrand factor (VWF), promotes lysis of arterial thrombi resistant to rtPA.[41] Thus, we investigated whether NAC could improve ischemic lesion size, recanalization and tissue reperfusion, risk of HTs, and neurological outcomes in hyperglycemic mice after stroke. We injected 400 mg/kg of NAC 20 minutes after occlusive thrombus formation in STZ-pretreated mice (Figure 3A). As expected, both rtPA and NAC, either alone or combined, increased the angiographic score measured by 7T MRI (STZ: 14% of complete recanalization; STZ-rtPA: 77%; STZ-NAC: 64%; STZ-NAC-rtPA: 79%; Figure 3D).

More interestingly, NAC significantly reduced ischemic lesion sizes in hyperglycemic mice (−33% in STZ-NAC group vs STZ group, $P < .05$, n = 14; Figure 3B-C), whereas rtPA alone showed no significant effect, consistent with prior reports (40.20 ± 9.5 mm^3 in STZ groups vs 40.43 ± 9.0 mm^3 in STZ-rtPA group, $P > .99$, n = 14). Moreover, rtPA did not reduce nor enhance NAC beneficial effects when coadministered (26.92 ± 14.3 mm^3 in STZ-NAC group vs 21.59 ± 10.7 mm^3 in STZ-NAC-rtPA group, $P = .58$, n = 14). The NAC-induced beneficial effect alone did not result in an increase in HTs, with 43% and 36% of petechial and parenchymal hemorrhage in the STZ and STZ-NAC groups, respectively (n = 14). This is in contrast to the effects observed with rtPA, either alone or combined with NAC, with which HTs were 64% in the STZ-rtPA group and 89% in the STZ-NAC-rtPA group (n = 14; Figure 3E). Accordingly, NAC treatment led to better functional outcomes when compared with rtPA alone. The functional recovery test at day 1 showed that the STZ-NAC group was significantly less affected by stroke than the untreated group in terms of the left/right ratio (0.84 ± 0.06 in STZ group vs 0.91 ± 0.05 in STZ-NAC group, n = 14, $P < .01$; Figure 3F). On day 3, the functional recuperation was better in groups treated with NAC concerning the left/right ratio, and both paws (0.87 ± 0.09 in STZ group vs 0.94 ± 0.05 in STZ-NAC and STZ-NAC-rtPA groups, n = 14, $P < .05$; Figure 4F; $84.3\% \pm 6.3\%$ in STZ group vs $94.2\% \pm 9.4\%$
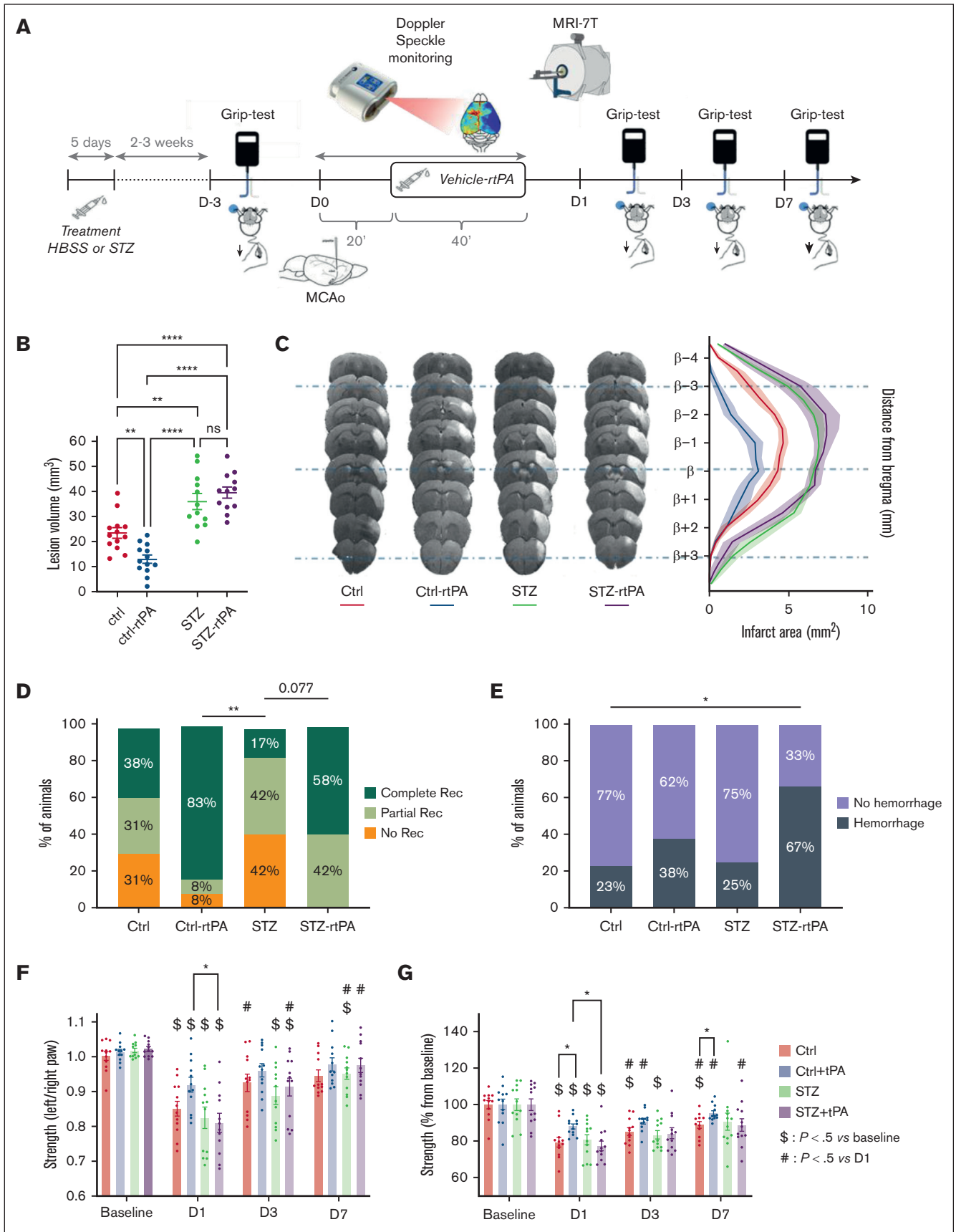
Figure 1.

in STZ-NAC group and 93.5% ± 6.0% in STZ-NAC-rtPA group, n = 14, $P < .05$; Figure 3G). On day 7, only animals treated with the combination of NAC and rtPA presented a better recovery than on day 1 for both parameters (Figure 3F-G). These data suggest that targeting VWF with NAC could be a relevant thrombolytic strategy for patients who have had a stroke, especially in the presence of a comorbidity such as chronic hyperglycemia in order to reduce the risk of HTs.

Targeting endothelial tPA-dependent NMDAR signaling increases the benefit of rtPA- or NAC-mediated thrombolysis

Some of the deleterious effects of exogenous rtPA and endogenous tPA after stroke are mediated by their ability to promote the activity of neuronal and/or endothelial NMDAR.[12,15,16] To prevent these side effects of rtPA/tPA, we generated a monoclonal antibody, named Glunomab, which blocks the interaction of tPA with the amino-terminal domain of the GluN1 subunit of NMDAR and subsequent signaling.[12] We investigated whether Glunomab alone or combined with rtPA may counteract the deleterious effects of tPA after ischemic stroke, first in nonhyperglycemic animals (Figure 4A). As expected, early intravenous administration of rtPA reduced the lesion size by 41% compared with that in nontreated animals (n = 12, $P < .05$; Figure 4B). Glunomab administered alone led to brain protection (−49%, n = 12, $P < .01$), which was also observed in conjunction with rtPA (−49%, n = 12, $P < .01$). rtPA treatment promoted superficial tissue reperfusion (−4% ± 36.0% of reperfusion in the Ctrl group compared with +57.3% ± 82.5% in the rtPA group, n = 12, $P < .05$ compared with the Ctrl group; supplemental Figure 4; Figure C) and recanalization at 24 hours (83% of partial and complete recanalization, n = 12; Figure 4C), either administered alone or combined with Glunomab (−4% ± 36.0% of reperfusion in Ctrl group compared with +48% ± 54.9% in Gluno-rtPA group, n = 12; supplemental Figure 4) and 92% of partial and complete recanalization at 24 hours, n = 12 for (Figure 4C). Glunomab alone improved recanalization at 24 hours (91% of partial and complete recanalization at 24 hours, n = 12; Figure 4C). Moreover, the beneficial effects induced by Glunomab were not associated with an increase in HTs, with 25% of petechial and parenchymal hemorrhage

observed for Glunomab alone, compared with 33% of total hemorrhages in the Ctrl group (Figure 4D).

In hyperglycemic animals (Figure 5A), the intravenous administration of rtPA failed to reduce the lesion size (−4% compared with STZ group, n = 15-16, $P = .99$; Figure 5B-C). However, coadministration of Glunomab and rtPA led to a significant reduction of lesion volumes (−46% in STZ-Gluno-rtPA group compared with STZ group, n = 15-16, $P < .01$, and −43% compared with rtPA alone, n = 15-16, $P < .01$; Figure 5B-C). Glunomab alone also demonstrated brain protection (−31%, n = 15-16, $P < .05$ when compared with only the STZ group; Figure 5B-C). The rtPA-mediated reperfusion/recanalization (+10% ± 14.1% for real-time tissue reperfusion compared with −1.1% ± 4.1% for STZ group, n = 15-16, $P < .05$; supplemental Figure 5B; and 57% of complete recanalization at 24 hours in the STZ-rtPA group, n = 15-16; Figure 5D) was associated with a higher rate of HTs (80% of animals with petechial and parenchymal hemorrhage in the STZ-rtPA group, n = 15; Figure 5E). The concurrent administration of Glunomab and rtPA demonstrated improved outcomes, with 67% achieving complete recanalization at 24 hours (n = 16; Figure 5E), a 9.2% increase in real-time tissue reperfusion compared with that in the STZ group (n = 16, $P < .05$; supplemental Figure 5B), and a 31% occurrence of petechial and parenchymal hemorrhage (n = 16; Figure 5E) compared with 31% in the STZ group. These improvements correlated with enhanced functional outcomes (Figure 5F-G). At day 7, Glunomab alone or its combination with either rtPA or NAC exhibited superior recovery compared with the STZ and STZ-rtPA groups, as indicated by the left/right paw strength ratio when compared with that on day 1 (at day 7: STZ, 0.93 ± 0.03; STZ-rtPA, 0.91 ± 0.05; STZ-Gluno, 0.96 ± 0.06; STZ-Gluno-rtPA, 0.96 ± 0.07; n = 15-16; $P < .05$; Figure 5F). Additionally, regarding the strength of both paws at day 7, the STZ-Gluno-rtPA group showed greater improvement than the STZ and STZ-rtPA groups (at day7: 97.1% ± 3.9% from the baseline in the STZ-Gluno-rtPA group, compared with 88.2% ± 5.2% from the baseline in the STZ group and 88.4% ± 6.1% in the STZ-rtPA group; n = 15-16; $P < .05$; Figure 5G). These findings suggest that the side effects of recombinant and endogenous tPA involve, at least in part, tPA-dependent endothelial NMDARs signaling.

Figure 1. Chronic hyperglycemia induces rtPA resistance and increases HT in a mouse model of thromboembolic stroke. (A) Schematic representation of the experimental protocol. (B) Quantification of ischemic lesion volume, 24 hours after MCAo assessed by T2-weighted imaging (7T MRI) in saline or rtPA treated (10 mg/kg; Actilyse, 10% bolus, 90% perfusion during 40 minutes) on nonhyperglycemic mice (Ctrl) or on hyperglycemic mice (STZ). Individual values, means, and standard error of the mean (SEM) are plotted; 23.38 mm^3 for Ctrl group (n = 13); 12.88 mm^3 for Ctrl-rtPA group (n = 13); 36 mm^3 for STZ group (n = 12); 39.58 mm^3 for STZ-rtPA group (n = 12). Ordinary 1-way analysis of variance (ANOVA) ($P < .01$); Tukey test for multiple comparisons (**$P < .01$; ****$P < .0001$). (C) Representative T2-weighted 7T MRI brain images (left) and representation of the lesion distribution around bregma (right), 24 hours after MCAo in Ctrl, Ctrl-rtPA, STZ, and STZ-rtPA groups. (D) Percentage of angiographic scores 24 hours after MCAo assessed by FLASH TOF 2D imaging (7T MRI) in Ctrl (n = 13), Ctrl-rtPA (n = 12), STZ (n = 12), and STZ-rtPA (n = 12) groups. No recanalization = complete occlusion (orange); partial recanalization = incomplete filling of the distal bed (light green); and complete recanalization = complete filling of the distal bed (dark green). Kruskal-Wallis test ($P < .01$); Dunns test for multiple comparisons (**$P < .01$). (E) Proportion of HT per groups, 24 hours after MCAo assessed by T2*-weighted imaging (deoxyhemoglobin; 7T MRI) in Ctrl (n = 13), Ctrl-rtPA (n = 13), STZ (n = 12), and STZ-rtPA (n = 12) groups. Fisher exact tests between groups (*$P < .05$). (F) Quantification of the specific left paw–strength deficit measured by grip-test ratio (strength of left/right paws) of Ctrl, Ctrl-rtPA, STZ, and STZ-rtPA groups (n = 12) before MCAo and on days 1, 3, and 7 after MCAo. Data were assessed in grams. Results are represented in mean ± SEM; 2-way ANOVA: time × group effect = 0.0211; Tukey test for multiple comparison (*$P < .05$ between groups at each time; $$P < .5$ vs baseline for each group: impact of Stroke; #$P < .5$ vs day 1 for each group: recovery). (G) Quantification of the global strength deficit measured by grip-test of forepaws of Ctrl, Ctrl-rtPA, STZ, and STZ-rtPA groups (n = 12) before and on days 1, 3, and 7 after MCAo. Data were assessed in grams and converted in percentage normalized for each animal with the corresponding baseline value (before MCAo). Results are represented in mean ± SEM; 2-way ANOVA: time factor <0.0001, and group factor <0.001; Tukey test for multiple comparison (*$P < .05$ between groups at each time; $$P < .5$ vs baseline for each group: impact of stroke; #$P < .5$ vs day 1 for each group: recovery).
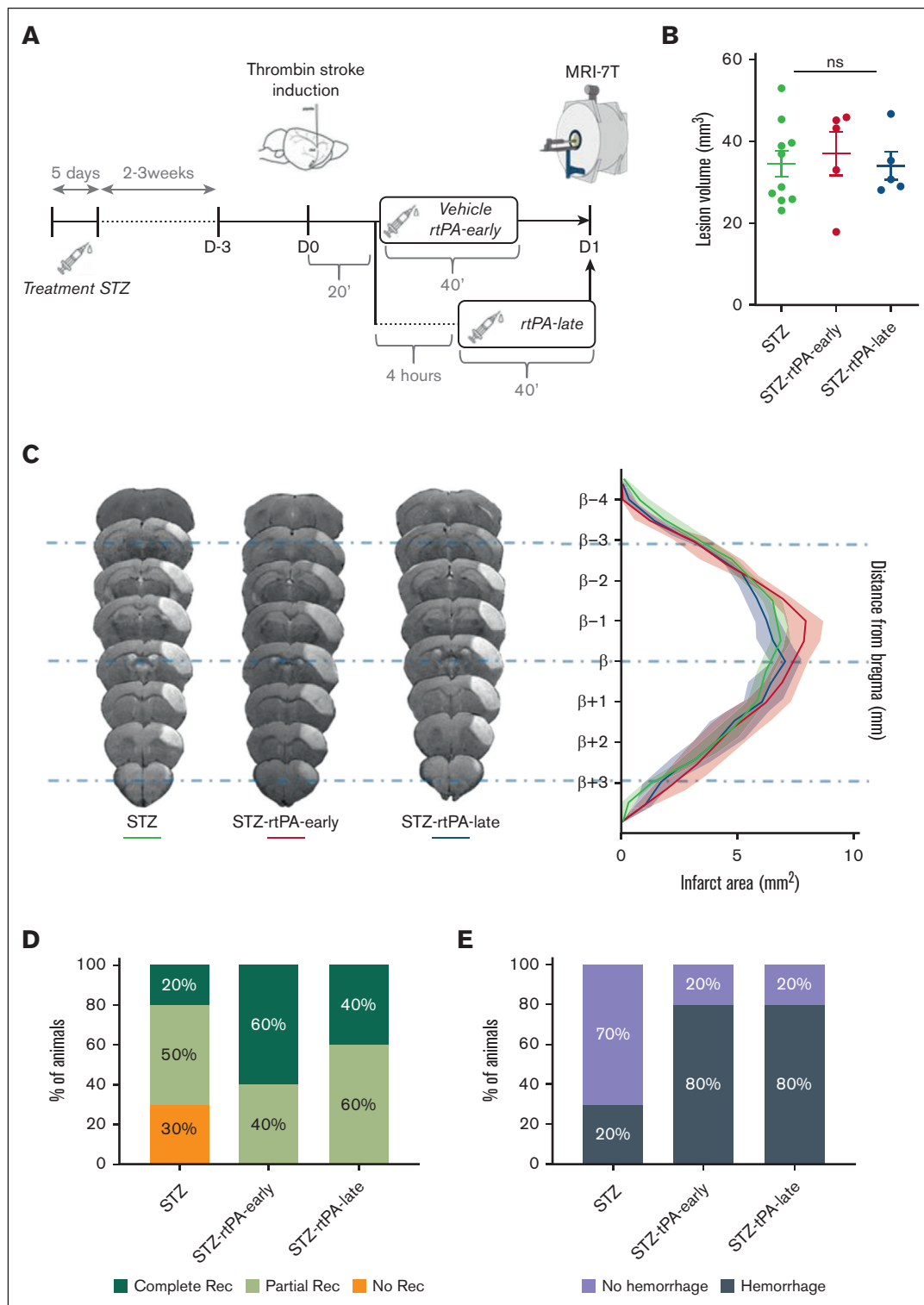
Figure 2. Chronic hyperglycemia induces rtPA resistance and increases HT independently of the therapeutic window. (A) Schematic representation of the experimental protocol. (B) Quantification of ischemic lesion volume, 24 hours after MCAo assessed by T2-weighted imaging (7T MRI) in hyperglycemic mice treated with saline (STZ group) or rtPA (10 mg/kg; Actilyse, 10% bolus, 90% perfusion during 40 minutes), in early 20 minutes after MCAo (STZ-rtPA-early) or in late 4 hours after MCAo (STZ-rtPA-late). Individual values, means, and SEM are plotted; 34.45 mm^3 for STZ group (n = 10); 37.01 mm^3 for STZ-rtPA-early group (n = 5); and 33.98 mm^3 for STZ-rtPA-late group (n = 5). Ordinary 1-way ANOVA ($P = .14$). (C) Representative T2-weighted 7T MRI brain images (left) and representation of the lesion distribution around bregma (right) 24 hours after MCAo in STZ, STZ-rtPA-early and STZ-rtPA-late groups. (D) Percentage of angiographic scores, 24 hours after MCAo assessed by FLASH_TOF_2D imaging (7T MRI) in STZ (n = 10), STZ-rtPA-early (n = 5), and STZ-rtPA-late (n = 5) groups. No recanalization = complete occlusion (orange); partial recanalization = incomplete filling of the distal bed (light green); and complete recanalization = complete filling of the distal bed (dark green). Kruskal-Wallis test ($P = .16$). (E) Proportion of HT per group, 24 hours after MCAo assessed by T2*-weighted imaging (deoxyhemoglobin; 7T MRI) in STZ (n = 10), STZ-rtPA-early (n = 5), and STZ-rtPA-late (n = 5) groups. Fisher exact tests between groups ($P > .05$).
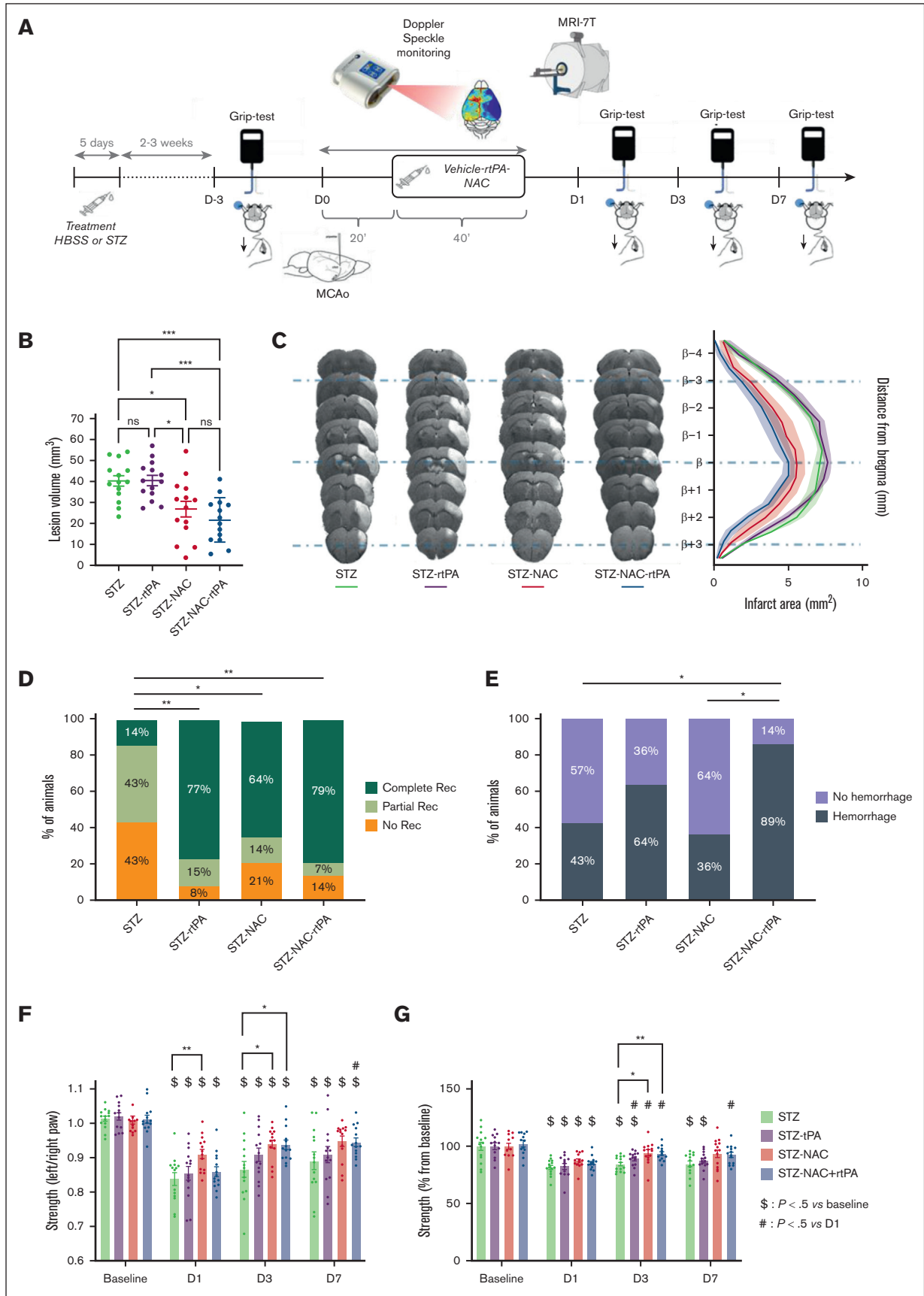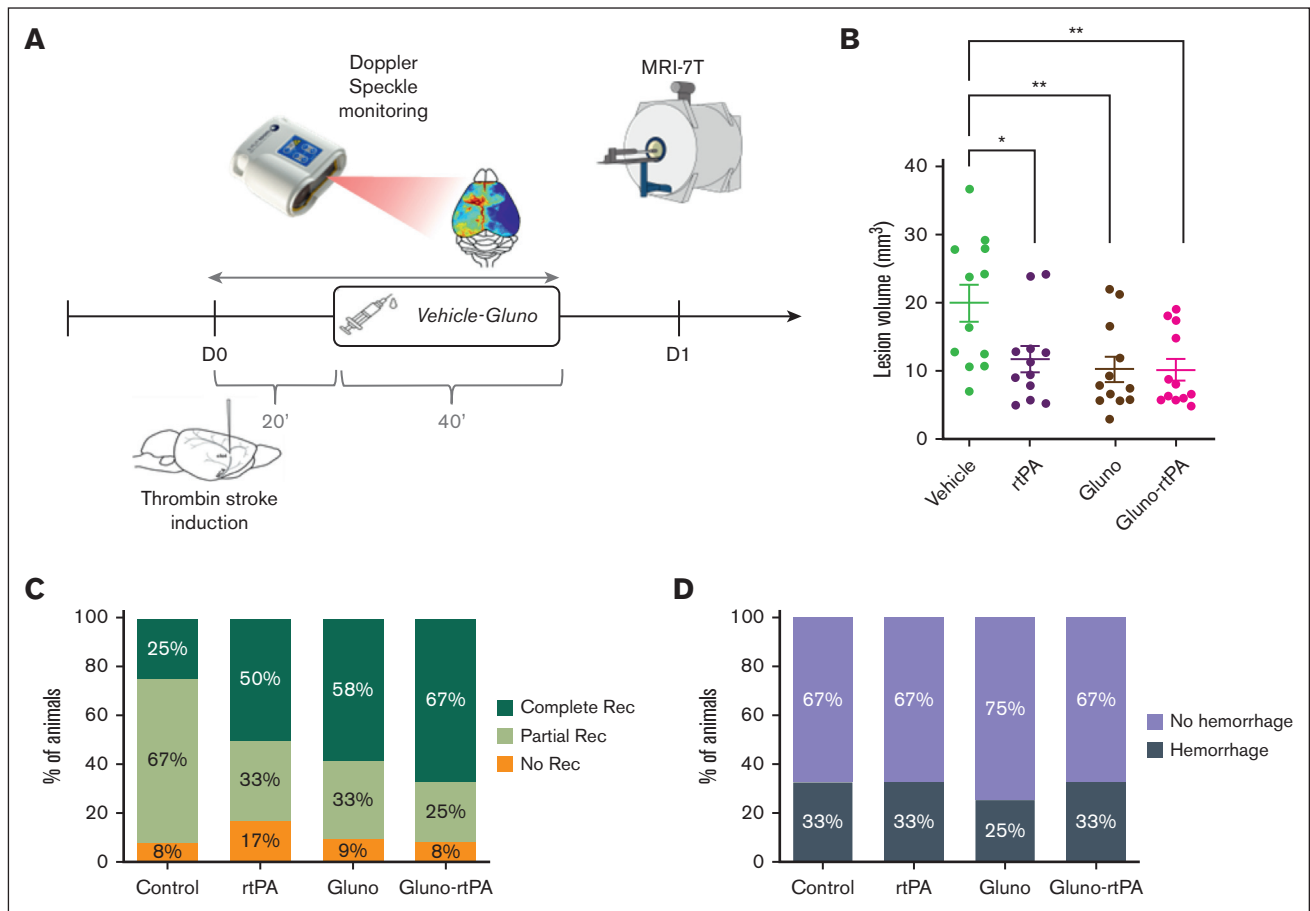
Figure 3.

Figure 4. Targeting endothelial tPA-dependent NMDAR signaling with Glunomab increases the benefit of rtPA-mediated thrombolysis in nonhyperglycemic mice. (A) Schematic representation of the experimental protocol. (B) Quantification of ischemic lesion volume, 24 hours after MCAo assessed by T2-weighted imaging (7T MRI) in mice treated with saline (vehicle group), rtPA (10 mg/kg; Actilyse, 10% bolus, 90% perfusion during 40 minutes; rtPA group), Glunomab (300 μg, 100% bolus; Gluno group), or a combination of Glunomab-rtPA (Gluno-rtPA group). Individual values, means and SEM are plotted. 21.57 mm³ for vehicle group (n = 12); 12.07 mm³ for tPA group (n = 12); 10.26 mm³ for Gluno group (n = 12); and 11.04 mm³ for Gluno-rtPA group (n = 12). Ordinary 1-way ANOVA ($P < .001$); Tukey test for multiple comparisons (*$P < .05$ and **$P < .01$). (C) Percentage of angiographic scores, 24 hours after MCAo assessed by FLASH_TOF_2D imaging (7T MRI) in vehicle, rtPA, Gluno, and Gluno-rtPA groups (n = 12 per group). No recanalization = complete occlusion (orange); partial recanalization = incomplete filling of the distal bed (light green); and complete recanalization = complete filling of the distal bed (dark green). Kruskal-Wallis test ($P = .33$). (D) Proportion of HT per group, 24 hours after MCAo assessed by T2*-weighted imaging (deoxyhemoglobin; 7T MRI) in vehicle, rtPA, Gluno, and Gluno-rtPA groups (n = 12 per group). Fisher exact tests between groups ($P > .05$).

Figure 3. N-Acetyl-Cysteine induces recanalization after acute thrombosis in chronically hyperglycemic animals without risk of HT. (A) Schematic representation of the experimental protocol. (B) Quantification of ischemic lesion volume 24 hours after MCAo assessed by T2-weighted imaging (7T MRI) in hyperglycemic mice treated after stroke with saline (STZ) or rtPA (10mg/kg; Actilyse, 10% bolus, 90% perfusion during 40 minutes; STZ-rtPA group), NAC (400 mg/kg, slow bolus during 60 seconds; STZ-NAC group) or a combination of NAC and rtPA (STZ-NAC-rtPA group). 40.20 mm³ for STZ group (n = 14); 40.43 mm³ for STZ-rtPA group (n = 14); 26.92 mm³ for STZ-NAC group (n = 14); 21.59 mm³ for STZ-NAC-rtPA group (n = 14). Ordinary one-way ANOVA ($P < .001$); Tukey test for multiple comparisons (*$P < .05$; ***$P < .001$). (C) Representative T2-weighted 7T MRI brain images (left) and representation of the lesion distribution around bregma (right) 24 hours after MCAo in STZ, STZ-rtPA, STZ-NAC and STZ-NAC-rtPA groups. (D) Percentage of angiographic scores 24 hours after MCAo assessed by FLASH_TOF_2D imaging (7T MRI) in STZ, STZ-rtPA, STZ-NAC and STZ-NAC-rtPA groups (n = 13-14 per group). No recanalization = complete occlusion (orange); partial recanalization = incomplete filling of the distal bed (light green); complete recanalization = complete filling of the distal bed (dark green). Kruskal-Wallis test ($P < .01$); Dunn's test for multiple comparisons (*$P < .05$, **$P < .01$). (E) Proportion of HT per groups 24 hours after MCAo assessed by T2*-weighted imaging (deoxyhemoglobin; 7T MRI) in STZ, STZ-rtPA, STZ-NAC and STZ-NAC-rtPA groups (n = 14 per group). Fisher exact tests between groups (*$P < .05$). (F) Quantification of the specific left paw strength deficit measured by grip-test ratio (strength of left/right paws) on day before and on day 1, day 3, and day 7 after MCAo in STZ, STZ-rtPA, STZ-NAC and STZ-NAC-rtPA groups (n = 14 per group). Data were assessed in grams. Results are represented in mean ± SEM. 2-way ANOVA: Time factor <0.0001 and group factor <0.001; Tukey test for multiple comparison (*$P < .05$ between groups at each time; $$P < .5$ vs baseline for each group: impact of Stroke; #$P < .5$ vs day 1 for each group: recovery). (G) Quantification of the global strength deficit measured by grip-test of forepaws before and on days 1, 3, and 7 after MCAo in STZ, STZ-rtPA, STZ-NAC and STZ-NAC-rtPA groups (n = 14 per group). Data were assessed in grams and converted in percentage normalized for each animal with the corresponding baseline value (before MCAo). Results are represented in mean ± SEM. 2-way ANOVA: Time factor <0.0001 and group factor <0.001; Tukey test for multiple comparison (*$P < .05$ between groups at each time; $$P < .5$ vs baseline for each group: impact of Stroke; #$P < .5$ vs day 1 for each group: recovery).
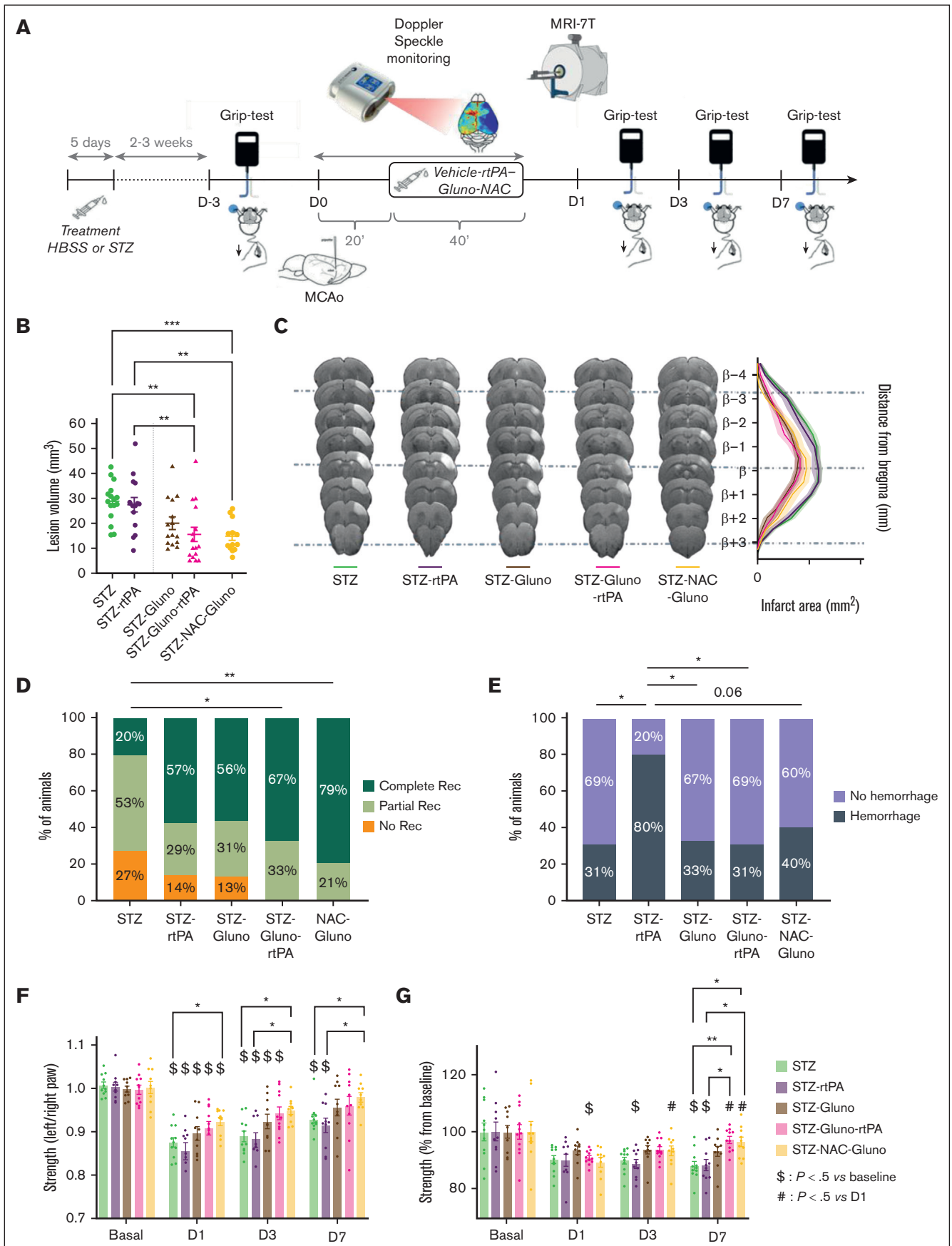
Figure 5.

We also tested Glunomab in combination with NAC in our model of thromboembolic stroke in hyperglycemic animals (Figure 5A). Early intravenous administration of NAC and Glunomab diminished the lesion size by 48% compared with nontreated STZ animals (n = 15-16; $P < .005$; Figure 5B-C) or rtPA-treated STZ animals (−46.2%; n = 15-16; $P < .01$; Figure 5B-C). Accordingly, NAC combined with Glunomab promoted 24-hour recanalization (79% of complete recanalization, n = 16; Figure 5D). These positive effects were accompanied by the absence of increased HTs (40% of petechial and parenchymal hemorrhage; Figure 5E), consistent with the observed enhancements in functional outcomes (Figure 5F-G). Concerning strength ratios at days 1, 3, and 7, the combination of NAC with Glunomab significantly provided better outcomes than in the STZ and STZ-rtPA groups (at day 1: STZ-NAC-Gluno, 0.92 ± 0.03; STZ, 0.87 ± 0.04; STZ-rtPA, 0.85 ± 0.06; $P < .05$; on day 3: STZ-NAC-Gluno, 0.95 ± 0.03; STZ, 0.89 ± 0.04; STZ-rtPA, 0.89 ± 0.04; $P < .05$; on day 7: STZ-NAC-Gluno, 0.98 ± 0.03; STZ, 0.93 ± 0.03; STZ-rtPA, 0.91 ± 0.05; n = 15-16; $P < .05$; Figure 5F). Moreover, concerning both paw strengths at day 7, we observed better midterm recuperation in the STZ-NAC-Gluno group than in the STZ and STZ-rtPA groups (at day 7: STZ-NAC-Gluno, 96.3% ± 5.5%; STZ, 88.2% ± 5.2%; STZ-rtPA, 88.4% ± 6.1%; n = 15-16 $P < .05$; Figure 5G).

Targeting endothelial tPA-dependent NMDAR signaling reduces infiltration of circulating inflammatory cells in the ischemic brain

Previous data have highlighted that Glunomab, by inhibiting the tPA-dependent interaction with endothelial NMDAR, effectively reduce immune cell migration across the BBB in both in vitro and in vivo settings.[12,15] We, thus, hypothesized that Glunomab might extend its therapeutic effects in stroke by reducing immune cell infiltration.[46] To investigate this, flow cytometry analyses were performed on brain tissues retrieved from nonhyperglycemic and hyperglycemic mice subjected to thromboembolic stroke, treated either with or without rtPA and Glunomab, at 5 days after stroke onset (n = 5-6; Figure 6A; supplemental Figure 6B). Notably, the

animals included in this analysis at 5 days after stroke displayed similar outcomes to those of which data are presented in the preceding figures measured at 24 hours after stroke, concerning lesion volumes, angiographic scores, HT, and real-time tissue reperfusion (n = 5-6; supplemental Figure 6A). We analyzed $CD11b^+/CD45^{low}$ microglial cells, $CD11b^+/CD45^{high}$ activated microglial cells or infiltrated macrophages, $CD11^+/CD45^+/Ly6G^+$ neutrophils, $CD3^+$ T cells, $CD8^+$ T cells, and $CD4^+$ T cells (Figure 6B-D; supplemental Figure 6B). As expected, ischemia led to increased inflammatory status in the ipsilateral hemisphere compared with the contralateral hemisphere for almost all analyzed cell types in untreated groups. Five days after stroke, levels of neutrophils and $CD8^+$ T cells were increased in the ipsilateral hemisphere of hyperglycemic mice, with or without rtPA treatment (n = 5-6; supplemental Figure 6B). Hyperglycemia also increased the infiltration of neutrophils and $CD8^+$ T cells in the ipsilateral hemisphere (+125% of neutrophil cells for STZ-rtPA−treated animals compared with Ctrl animals, $P < .05$, and +76% of $CD8^+$ T cells for STZ-rtPA−untreated animals compared with control, $P < 0,1$, n = 5-6; Figure 6C-E). The administration of Glunomab significantly reduced the infiltration of both cells type, especially when combined with rtPA. Specifically, we observed a reduction of invading neutrophils of 126% in STZ animals treated with the combination of Glunomab and rtPA compared with those treated with rtPA ($P < .05$; Figure 6C). Additionally, there was a beneficial effect of Glunomab in STZ animals regarding $CD3^+CD8^+$ T-cell population, with a 74% reduction in invading cytotoxic T cells in STZ-rtPA-Gluno mice compared with STZ mice. These findings indicate that the beneficial effects of Glunomab on different stroke outcomes are associated with reduced invasion of brain tissue by circulating inflammatory cells.

In a thromboembolic experimental stroke model responsive to rtPA treatment, our data reveal that hyperglycemia not only impairs the efficacy of the gold-standard treatment but also amplifies the risk of rtPA-associated HTs and exacerbates inflammatory responses. These side effects appear to be mediated through the tPA-dependent endothelial NMDAR signaling.

Figure 5. Glunomab coupled with a thrombolytic agent improves stroke outcome and protects against HT in chronically hyperglycemic animals. (A) Schematic representation of the experimental protocol. (B) Quantification of ischemic lesion volume, 24 hours after MCAo assessed by T2-weighted imaging (7T MRI) in mice treated with saline (STZ group), rtPA (10mg/kg; Actilyse, 10% bolus, 90% perfusion over 40 minutes; and STZ-rtPA group), Glunomab (300 μg, 100% bolus; STZ-Gluno group), a combination of Glunomab and rtPA (STZ-Gluno-rtPA group), and a combination of Glunomab and NAC (400 mg/kg, slow bolus) on hyperglycemic mice. Individual values, means, and SEM are plotted; 28.80 mm³ for STZ group (n = 16); 27.66 mm³ for STZ-rtPA group (n = 15); 20.14 mm³ for STZ-Gluno group (n = 15); 15.64 mm³ for STZ-Gluno-rtPA group (n = 16); and 14.88 mm³ for STZ-NAC-Gluno group (n = 15). Ordinary 1-way ANOVA ($P < .001$); Tukey multiple comparisons (**$P < .01$ and ***$P < .001$). (C) Representative T2-weighted 7T MRI brain images (left) and representation of the lesion distribution around bregma (right), 24 hours after MCAo in STZ, STZ-rtPA, STZ-Gluno, STZ-Gluno-rtPA, and STZ-NAC-Gluno groups. (D) Percentage of angiographic scores, 24 hours after MCAo assessed by FLASH_TOF_2D imaging (7T MRI) in STZ (n = 15), STZ-rtPA (n = 14), STZ-Gluno (n = 15), STZ-Gluno-rtPA (n = 15), and STZ-Gluno-NAC (n = 14) groups. No recanalization = complete occlusion (orange); partial recanalization = incomplete filling of the distal bed (light green); and complete recanalization = complete filling of the distal bed (dark green). Kruskal-Wallis test ($P < .05$); Dunns test for multiple comparisons (*$P < .01$ and **$P < .01$). (E) Proportion of HT per groups, 24 hours after MCAo assessed by T2*-weighted imaging (deoxyhemoglobin; 7T MRI) in STZ (n = 16), STZ-rtPA (n = 15), STZ-Gluno (n = 15), STZ-Gluno-rtPA (n = 16), and STZ-Gluno-NAC (n = 15) groups. Fisher exact tests between groups (*$P < .05$). (F) Quantification of the specific left paw−strength deficit measured by grip-test ratio (strength of left/right paws) of STZ (n = 16), STZ-rtPA (n = 15), STZ-Gluno (n = 15), STZ-Gluno-rtPA (n = 16), and STZ-Gluno-NAC (n = 15) groups, 1 day before, and on day 1, day 3, and day 7 after MCAo. Data were assessed in grams. Results are represented in mean ± SEM; 2-way ANOVA: time effect <0.0001 and group effect <0.01; Tukey test for multiple comparison (*$P < .05$ between groups at each time; $$P < .5$ vs baseline for each group: impact of Stroke; #$P < .5$ vs day 1 for each group: recovery). (G) Quantification of the global strength deficit measured by grip-test of forepaws of STZ (n = 16), STZ-rtPA (n = 15), STZ-Gluno (n = 15), STZ-Gluno-rtPA (n = 16), and STZ-Gluno-NAC (n = 15) groups 1 day before and on day 1, day 3, and day 7 after MCAo. Data were assessed in grams and converted in percentage normalized for each animal with the corresponding baseline value (before MCAo). Results are represented in mean ± SEM; 2-way ANOVA: time factor <0.0001; Tukey test for multiple comparison (*$P < .05$ between groups at each time; $$P < .5$ vs baseline for each group: impact of Stroke; #$P < .5$ vs day 1 for each group: recovery).

Figure 6. Targeting endothelial tPA-dependent NMDAR signaling with Glunomab reduces invasion of the ischemic brain tissues by circulating inflammatory cells. (A) Schematic representation of the experimental protocol. (B) Representative flow cytometry dot plots and gating strategy used for quantification of CD11b$^+$CD45^{low} microglia, CD11b$^+$CD45^{hi} activated microglia or macrophages and CD11b$^+$CD45$^+$Ly6G$^+$ neutrophils, 5 days after stroke in ipsilateral mice brain. (C) Flow cytometry quantification of microglia, activated microglia or macrophages, and neutrophils 5 days after stroke in ipsilateral mice brain in the Ctrl group (n = 6), STZ group (n = 5), STZ-rtPA group (n = 5), STZ-Gluno group (n = 5), and STZ-Gluno-rtPA group (n = 5); *P < .05; ordinary 1-way ANOVA; Tukey multiple comparisons. (D) Representative flow cytometry dot plots and gating strategy used for quantification of CD3$^+$ T cells, CD3$^+$CD8$^+$ cytotoxic T cells, and CD3$^+$CD4$^+$ regulatory/helper T cells, 5 days after stroke in ipsilateral mice brain. (E) Flow cytometry quantification of CD3$^+$ T cells, CD3$^+$CD8$^+$ cytotoxic T cells, and CD3$^+$CD4$^+$ regulatory/helper T cells, 5 days after stroke in ipsilateral mice brain in the Ctrl group (n = 6), STZ group (n = 5), STZ-rtPA group (n = 5), STZ-Gluno group (n = 5), and STZ-Gluno-rtPA group (n = 5); *P < .05; ordinary 1-way ANOVA; Tukey multiple comparisons.
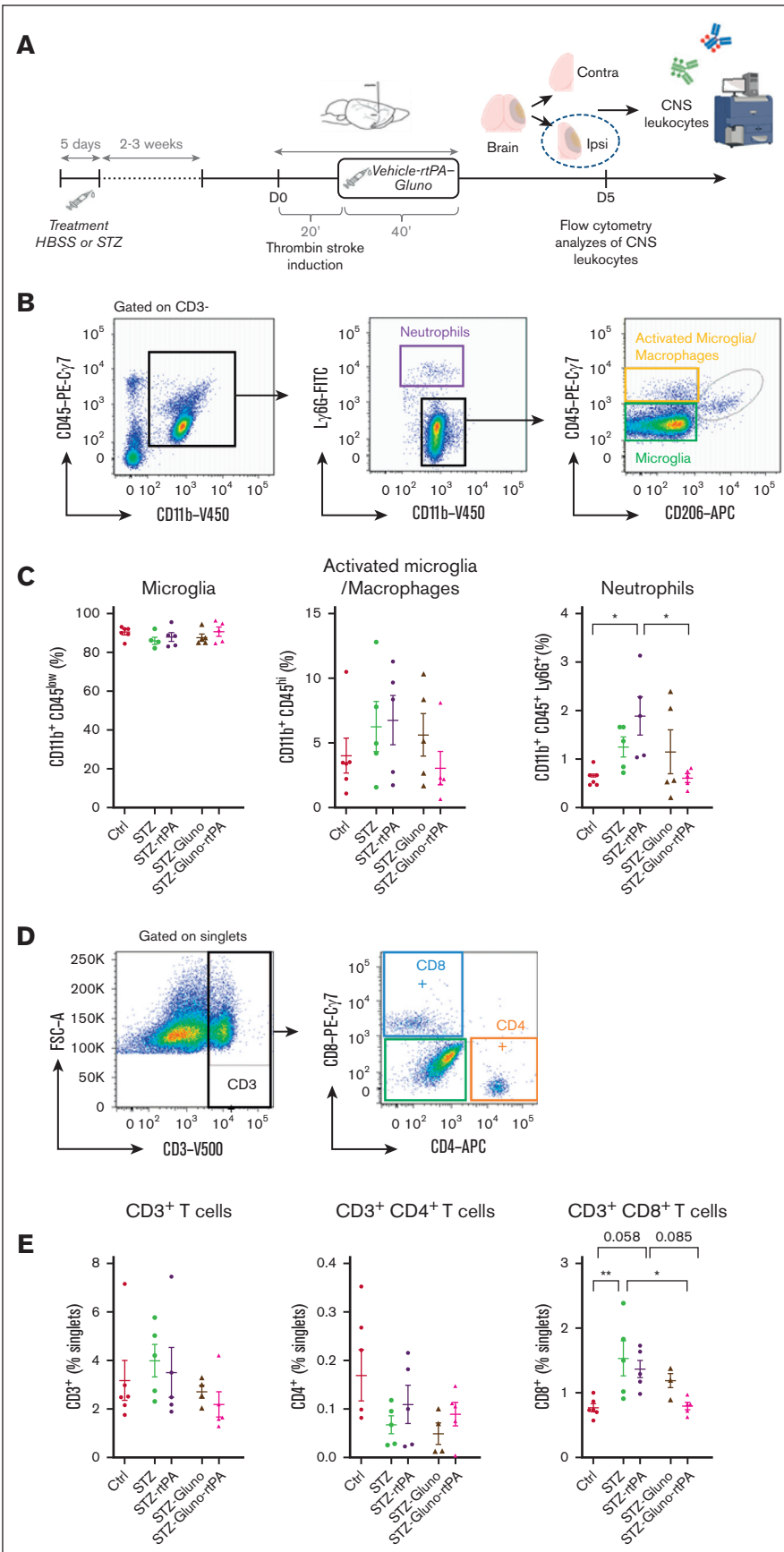
Discussion

Hyperglycemia is a prevalent comorbidity among stroke patients, affecting up to 50% of individuals.[47,48] It is characterized by elevated serum glucose levels and correlates with larger lesion volumes and more severe deficits. Furthermore, hyperglycemia increases the risk of recurrent ischemic stroke, especially after a transient ischemic attack or minor stroke.[49]

In this study, we evaluated the efficacy and safety of 2 thrombolytic agents: the well-established rtPA (Alteplase/Actilyse) and NAC. Prior research has highlighted the beneficial effects of NAC after stroke by dissolving rtPA-resistant clots.[50-54] This effect is achieved through NAC's targeting of VWF present in platelet-rich clots.[41] Administration of all drugs occurred 20 minutes after the onset of stroke, consistent with the previously estimated therapeutic window of 90 minutes for the preclinical model used in our study.[4,41]

When conducted in animals without comorbidities, the thromboembolic stroke model induced by thrombin results in the formation of a fibrin-rich clot that remains responsive to rtPA treatment.[4] Notably, there is no clear evidence of significant HTs or moderation when tPA is administered at a later stage.[4,5,55,56] Our metaanalysis, encompassing various studies, supports the idea that, in this model, the administration of tPA does not substantially elevate the risk of HTs when comorbidities are absent. Consequently, this model enabled us to observe improved outcomes with interventions like NAC-targeting VWF[41,53,57] or a novel fibrinolytic agent called Microlyse, created through the combination of an antibody targeting fibrin and urokinase.[58]

In this preclinical investigation, chronic hyperglycemia has been observed to transform clots initially responsive to rtPA into partially rtPA-resistant clots. This transformation exacerbates the outcomes of stroke by increasing the occurrence of HTs and promoting inflammatory processes. Similar experiments have been carried out in our laboratory using female mice, revealing that chronic hyperglycemia results in larger lesions and more frequent HTs, with no discernible beneficial effects of tPA observed (data not shown).

This study demonstrates that NAC effectively dissolve clots that are partially resistant to rtPA, without increasing HTs, even in the presence of hyperglycemia. These findings gain further clinical significance from previous reports indicating NAC's positive outcomes in patients treated with streptokinase and nitroglycerine with acute myocardial infarction. These patients experienced improved outcomes linked to a faster coronary reperfusion rate in NAC-treated individuals (−39%).[59,60]

There are several sources of tPA: the endogenous tPA produced by endothelial cells,[61] hepatocytes,[62] and neurons,[63] as well as the exogenous tPA administered intravenously after stroke. Both forms of tPA exert influence on NMDAR signaling in neurons and endothelial cells.[64] tPA is known to influence neuronal death in pathological conditions and to modulate inflammatory processes and the integrity of the BBB, thus favoring HTs. These effects largely stem from tPA's ability to modulate neuronal and endothelial NMDAR signaling.[12,16]

Then, our hypothesis was that blocking the NMDAR/tPA interaction would enhance outcomes after stroke. To interrupt tPA-dependent endothelial NMDAR signaling, we used Glunomab, a monoclonal antibody that competes with both endogenous and exogenous tPA (administered via intravenous injection) for binding to the GluN1 subunit of NMDAR. In this context, Glunomab shows promise in alleviating tPA's side effects, including the risk of HT. Importantly, whether used alone (targeting endogenous tPA) or in combination with exogenous rtPA or NAC, Glunomab reduces ischemic lesion volumes and the infiltration of inflammatory cells into the injured brain tissue. These actions contribute to an enhanced functional recovery. As previously reported, NAC appears to demonstrate a more efficient and safer profile than rtPA as a thrombolytic agent after a stroke, a characteristic that is further strengthened in the presence of Glunomab.[41]

The brain hosts various resident immune cell subsets that contribute to inflammation upon activation after ischemic stroke.[46,65,66] Additionally, circulating macrophages, neutrophils, and T cells can cross the injured BBB[67-69] and reach the brain parenchyma.[46,70,71] Based on a previous study,[72] our investigation assessed the presence of these different cell types on different treatment conditions, 5 days after stroke onset. As expected, stroke exacerbates the inflammatory status of the injured brain parenchyma, a phenomenon worsened by chronic hyperglycemia and exposure to rtPA. As demonstrated previously in a preclinical model of multiple sclerosis,[73] Glunomab reduces the infiltration of CD8+ T cells and neutrophils.

These findings align with the established concept that modulating the dysregulated immune response can effectively promote poststroke brain recovery. Importantly, Glunomab does not directly target inflammatory cells but rather limits their passage through the endothelium of the BBB. This action is likely to reduce the risk of secondary detrimental effects.[46]

tPA is also considered as a cytokine-like molecule and a neuromodulator,[63,74] and these additional functions are partly attributed to its ability to modulate NMDAR signaling in neurons and endothelial cells.[12,15,16,73] Our present work sheds light on the direct contribution of tPA-dependent NMDAR signaling to both the infiltration of inflammatory cells across the BBB and the occurrence of HTs.

This study has several limitations. Firstly, human thrombi might exhibit distinct structures and greater variability compared with those replicated in our preclinical models. However, we consider our thromboembolic model as closely mimicking clinical scenarios. Secondly, despite its relevance, the STZ-induced model of chronic hyperglycemia does not fully replicate the clinical situation of diabetes.[43,75,76] In humans, hyperglycemia is defined as a blood glucose level of ≥180 mg/dL, whereas our preclinical model represents a situation of severe hyperglycemia (≥300 mg/dL).[49]

Additional preclinical data and clinical trials are required to establish the efficacy of targeting tPA-dependent endothelial NMDAR in patients who have experienced a stroke. It is important to note that both endogenous and exogenous tPA interact with endothelial NMDAR, suggesting that this strategy may be relevant not only for patients treated with rtPA but also for those receiving its derivatives, such as tenecteplase, which also interacts with NMDAR.[77]

Acknowledgments

Authorship

Contribution: F.L., C.O., N.V., and D.V. conceived the study; F.L., D.L., E.L., M.Y., J.F., F.P., and P.M. designed and performed experiments, and analyzed data; F.L. interpreted the results; F.L. and D.V. wrote the manuscript; F.L., M.B., B.H., M.R., A.L., and N.V. contributed to discussions and edited the manuscript; and all authors read and approved the manuscript.

Conflict-of-interest disclosure: The patent protecting Gluno-mab, the monoclonal antibody used in this study, is under exclusive license to Lys Therapeutics. D.V. is a coauthor of this patent; has been a speaker for Lys Therapeutics on topics related to this work; is the current president of the scientific committee of Lys Therapeutics; and is scientific adviser for STROK@LLIANCE (Caen, France). M.B. is cofounder and chief executive officer of Lys Therapeutics. F.P. and F.L. are employees of Lys Therapeutics. The remaining authors declare no competing financial interests.

ORCID profiles: F. Lebrun, 0000-0001-9577-2481; D.L., 0000-0002-7275-3170; M.Y., 0000-0001-8571-6021; F.P., 0009-0002-3387-3409; F. Lesept, 0000-0002-7398-9652; M.B., 0000-0003-3558-212X; M.R., 0000-0002-6120-4053; N.V., 0000-0002-7556-6004; D.V., 0000-0002-7636-2185.

Correspondence: Denis Vivien, Normandie University, UNI-CAEN, INSERM UMR-S U1237, Physiopathology and Imaging of Neurological Disorders, GIP Cyceron, Institute Blood and Brain @ Caen-Normandie, Blvd Becquerel, BP 5229, 14074 Caen Cedex, France; email: vivien@cyceron.fr.

References

1. Roaldsen MB, Lindekleiv H, Mathiesen EB. Intravenous thrombolytic treatment and endovascular thrombectomy for ischaemic wake-up stroke. *Cochrane Database Syst Rev*. 2021;12:CD010995.

2. Katsanos AH, Safouris A, Sarraj A, et al. Intravenous thrombolysis with tenecteplase in patients with large vessel occlusions: systematic review and meta-analysis. *Stroke*. 2021;52(1):308-312.

3. Warburton E, Alawneh JA, Clatworthy PL, Morris RS. Stroke management. *BMJ Clin Evid*. 2011;2011:0201.

4. Orset C, Haelewyn B, Allan SM, et al. Efficacy of alteplase in a mouse model of acute ischemic stroke: a retrospective pooled analysis. *Stroke*. 2016;47(5):1312-1318.

5. Orset C, Macrez R, Young AR, et al. Mouse model of in situ thromboembolic stroke and reperfusion. *Stroke*. 2007;38(10):2771-2778.

6. Sandset EC, Tsivgoulis G. Tenecteplase for acute ischaemic stroke. *Lancet*. 2022;400(10347):138-139.

7. Kaesmacher J, Mordasini P, Arnold M, et al. Direct mechanical thrombectomy in tPA-ineligible and -eligible patients versus the bridging approach: a meta-analysis. *J Neurointerv Surg*. 2019;11(1):20-27.

8. Wang DT, Churilov L, Dowling R, Mitchell P, Yan B. Successful recanalization post endovascular therapy is associated with a decreased risk of intracranial haemorrhage: a retrospective study. *BMC Neurol*. 2015;15(1):185.

9. L L Yeo L, Sharma VK. The quest for arterial recanalization in acute ischemic stroke-the past, present and the future. *J Clin Med Res*. 2013;5(4):251-265.

10. Kaesmacher J, Giarrusso M, Zibold F, et al. Rates and quality of preinterventional reperfusion in patients with direct access to endovascular treatment. *Stroke*. 2018;49(8):1924-1932.

11. Tissue plasminogen activator for acute ischemic stroke. *N Engl J Med*. 1995;333:1581-1588.

12. Lesept F, Chevilley A, Jezequel J, et al. Tissue-type plasminogen activator controls neuronal death by raising surface dynamics of extrasynaptic NMDA receptors. *Cell Death Dis*. 2016;7(11):e2466.e2466.

13. Chevilley A, Lesept F, Lenoir S, Ali C, Parcq J, Vivien D. Impacts of tissue-type plasminogen activator (tPA) on neuronal survival. *Front Cell Neurosci*. 2015;9:415.

14. Parcq J, Bertrand T, Montagne A, et al. Unveiling an exceptional zymogen: the single-chain form of tPA is a selective activator of NMDA receptor-dependent signaling and neurotoxicity. *Cell Death Differ*. 2012;19(12):1983-1991.

15. Mehra A, Guérit S, Macrez R, et al. Nonionotropic action of endothelial NMDA receptors on blood–brain barrier permeability via Rho/ROCK-mediated phosphorylation of myosin. *J Neurosci*. 2020;40(8):1778-1787.

16. Macrez R, Ortega MC, Bardou I, et al. Neuroendothelial NMDA receptors as therapeutic targets in experimental autoimmune encephalomyelitis. *Brain*. 2016;139(pt 9):2406-2419.

17. Fredriksson L, Lawrence D, Medcalf R. tPA modulation of the blood–brain barrier: a unifying explanation for the pleiotropic effects of tPA in the CNS. *Semin Thromb Hemost*. 2017;43(2):154-168.

18. Drieu A, Levard D, Vivien D, Rubio M. Anti-inflammatory treatments for stroke: from bench to bedside. *Ther Adv Neurol Disord*. 2018;11:1756286418789854.

19. Nicole O, Docagne F, Ali C, et al. The proteolytic activity of tissue-plasminogen activator enhances NMDA receptor-mediated signaling. *Nat Med*. 2001;7(1):59-64.

20. Samson AL, Ju L, Ah Kim H, et al. MouseMove: an open source program for semi-automated analysis of movement and cognitive testing in rodents. *Sci Rep*. 2015;5:16171.

21. Kvajo M, Albrecht H, Meins M, et al. Regulation of brain proteolytic activity is necessary for the in vivo function of NMDA receptors. *J Neurosci*. 2004; 24(43):9734-9743.

22. Lopatkiewicz AM, Gradek-Kwinta E, Czyzycki M, Pera J, Slowik A, Dziedzic T. Glucocorticoid resistance is associated with poor functional outcome after stroke. *Cell Mol Neurobiol*. 2020;40(8):1321-1326.

23. Iglesias-Rey R, da Silva-Candal A, Rodríguez-Yáñez M, et al. Neurological instability in ischemic stroke: relation with outcome, latency time, and molecular markers. *Transl. Stroke Res*. 2022;13(2):228-237.

24. Rezaeitalab F, Esmaeili M, Saberi A, et al. Predictive value of inflammatory markers for functional outcomes in patients with ischemic stroke. *Curr J Neurol*. 2020;19(2):47-52.

25. Sturgeon JD, Folsom AR, Longstreth WT, Shahar E, Rosamond WD, Cushman M. Hemostatic and inflammatory risk factors for intracerebral hemorrhage in a pooled cohort. *Stroke*. 2008;39(8):2268-2273.

26. Tschoe C, Bushnell CD, Duncan PW, Alexander-Miller MA, Wolfe SQ. Neuroinflammation after intracerebral hemorrhage and potential therapeutic targets. *J Stroke*. 2020;22(1):29-46.

27. Saand AR, Yu F, Chen J, Chou SH-Y. Systemic inflammation in hemorrhagic strokes - a novel neurological sign and therapeutic target? *J Cereb Blood Flow Metab*. 2019;39(6):959-988.

28. Shi K, Zou M, Jia D-M, et al. tPA mobilizes immune cells that exacerbate hemorrhagic transformation in stroke. *Circ Res*. 2021;128(1):62-75.

29. Chu Y-W, Chen P-Y, Lin S-K. Correlation between immune-inflammatory markers and clinical features in patients with acute ischemic stroke. *Acta Neurol Taiwan*. 2020;29(4):103-113.

30. Boehme AK, Kapoor N, Albright KC, et al. Systemic inflammatory response syndrome in tPA treated patients is associated with worse short-term functional outcome. *Stroke*. 2013;44(8):2321-2323.

31. Seillier C, Hélie P, Petit G, et al. Roles of the tissue-type plasminogen activator in immune response. *Cell Immunol*. 2022;371:104451.

32. Zhang C, Brandon NR, Koper K, Tang P, Xu Y, Dou H. Invasion of peripheral immune cells into brain parenchyma after cardiac arrest and resuscitation. *Aging Dis*. 2018;9(3):412-425.

33. Tsivgoulis G, Katsanos AH, Mavridis D, et al. Association of baseline hyperglycemia with outcomes of patients with and without diabetes with acute ischemic stroke treated with intravenous thrombolysis: a propensity score-matched analysis from the SITS-ISTR Registry. *Diabetes*. 2019;68(9): 1861-1869.

34. MacDougall NJJ, Muir KW. Hyperglycaemia and infarct size in animal models of middle cerebral artery occlusion: systematic review and meta-analysis. *J Cereb Blood Flow Metab*. 2011;31(3):807-818.

35. Navarro-Oviedo M, Roncal C, Salicio A, et al. MMP10 promotes efficient thrombolysis after ischemic stroke in mice with induced diabetes. *Transl Stroke Res*. 2019;10(4):389-401.

36. Dietrich WD, Alonso O, Busto R. Moderate hyperglycemia worsens acute blood-brain barrier injury after forebrain ischemia in rats. *Stroke*. 1993;24(1): 111-116.

37. McBride DW, Legrand J, Krafft PR, et al. Acute hyperglycemia is associated with immediate brain swelling and hemorrhagic transformation after middle cerebral artery occlusion in rats. *Acta Neurochir Suppl*. 2016;121:237-241.

38. Lo JW, Crawford JD, Samaras K, et al. Association of prediabetes and type 2 diabetes with cognitive function after stroke. *Stroke*. 2020;51(6): 1640-1646.

39. Jiang Y, Han J, Spencer P, et al. Diabetes mellitus: a common comorbidity increasing hemorrhagic transformation after tPA thrombolytic therapy for ischemic stroke. *Brain Hemorrhages*. 2021;2(3):116-123.

40. Ergul A, Kelly-Cobbs A, Abdalla M, Fagan SC. Cerebrovascular complications of diabetes: focus on stroke. *Endocr Metab Immune Disord Drug Targets*. 2012;12(2):148-158.

41. Martinez de Lizarrondo S, Gakuba C, Herbig BA, et al. Potent thrombolytic effect of N-acetylcysteine on arterial thrombi. *Circulation*. 2017;136(7): 646-660.

42. Arora S, Ojha SK, Vohora D. Characterisation of streptozotocin induced diabetes mellitus in swiss albino mice. *Global J Pharmacol*. 2009:81-84.

43. Furman BL. Streptozotocin-induced diabetic models in mice and rats. *Curr Protoc Pharmacol*. 2015;70(1):5.47.1-5.47.20.

44. Deeds MC, Anderson JM, Armstrong AS, et al. Single dose streptozotocin-induced diabetes: considerations for study design in islet transplantation models. *Lab Anim*. 2011;45(3):131-140.

45. Peña I dela, Borlongan C, Shen G, Davis W. Strategies to extend thrombolytic time window for ischemic stroke treatment: an unmet clinical need. *J Stroke*. 2017;19(1):50-60.

46. Drieu A, Buendia I, Levard D, et al. Immune responses and anti-inflammatory strategies in a clinically relevant model of thromboembolic ischemic stroke with reperfusion. *Transl Stroke Res*. 2020;11(3):481-495.

47. McCormick MT, Muir KW, Gray CS, Walters MR. Management of hyperglycemia in acute stroke. *Stroke*. 2008;39(7):2177-2185.

48. Lindsberg PJ, Roine RO. Hyperglycemia in acute stroke. *Stroke*. 2004;35(2):363-364.

49. Mac Grory B, Piccini JP, Yaghi S, et al. Hyperglycemia, risk of subsequent stroke, and efficacy of dual antiplatelet therapy: a post hoc analysis of the POINT Trial. *J Am Heart Assoc.* 2022;11(3):e023223.

50. Cuzzocrea S, Mazzon E, Costantino G, et al. Beneficial effects of n-acetylcysteine on ischaemic brain injury. *Br J Pharmacol.* 2000;130(6):1219-1226.

51. Karuppagounder SS, Alin L, Chen Y, et al. N-acetylcysteine targets 5 lipoxygenase-derived, toxic lipids and can synergize with prostaglandin E2 to inhibit ferroptosis and improve outcomes following hemorrhagic stroke in mice. *Ann Neurol.* 2018;84(6):854-872.

52. Khan M, Sekhon B, Jatana M, et al. Administration of N-acetylcysteine after focal cerebral ischemia protects brain and reduces inflammation in a rat model of experimental stroke. *J Neurosci Res.* 2004;76(4):519-527.

53. Sabetghadam M, Mazdeh M, Abolfathi P, Mohammadi Y, Mehrpooya M. Evidence for a beneficial effect of oral N-acetylcysteine on functional outcomes and inflammatory biomarkers in patients with acute ischemic stroke. *Neuropsychiatr Dis Treat.* 2020;16:1265-1278.

54. von Kummer R, Mori E, Truelsen T, et al. Desmoteplase 3 to 9 hours after major artery occlusion stroke: the DIAS-4 Trial (Efficacy and Safety Study of Desmoteplase to Treat Acute Ischemic Stroke). *Stroke.* 2016;47(12):2880-2887.

55. Anfray A, Brodin C, Drieu A, et al. Single- and two- chain tissue type plasminogen activator treatments differentially influence cerebral recovery after stroke. *Exp Neurol.* 2021;338:113606.

56. van Moorsel MVA, de Maat S, Vercruysse K, et al. VWF-targeted thrombolysis to overcome rh-tPA resistance in experimental thrombotic stroke models. *Blood.* 2022;140(26):2844-2848.

57. Uemura T, Watanabe K, Ko K, et al. Protective effects of brain infarction by N-acetylcysteine derivatives. *Stroke.* 2018;49(7):1727-1733.

58. de Maat S, Clark CC, Barendrecht AD, et al. Microlyse: a thrombolytic agent that targets VWF for clearance of microvascular thrombosis. *Blood.* 2022;139(4):597-607.

59. Marenco JP, Frye RE. *The clinical use of N-acetylcysteine in cardiology. The Therapeutic Use of N-Acetylcysteine (NAC) in Medicine.* Springer; 2019:277-287.

60. Sochman J. N-acetylcysteine in acute cardiology: 10 years later: what do we know and what would we like to know?!. *J Am Coll Cardiol.* 2002;39(9):1422-1428.

61. Furon J, Yetim M, Pouettre E, et al. Blood tissue plasminogen activator (tPA) of liver origin contributes to neurovascular coupling involving brain endothelial N-methyl-D-aspartate (NMDA) receptors. *Fluids Barriers CNS.* 2023;20(1):11.

62. Zheng Z, Nayak L, Wang W, et al. An ATF6-tPA pathway in hepatocytes contributes to systemic fibrinolysis and is repressed by DACH1. *Blood.* 2019;133(7):743-753.

63. Lenoir S, Varangot A, Lebouvier L, Galli T, Hommet Y, Vivien D. Post-synaptic release of the neuronal tissue-type plasminogen activator (tPA). *Front Cell Neurosci.* 2019;13:164.

64. Thiebaut AM, Gauberti M, Ali C, et al. The role of plasminogen activators in stroke treatment: fibrinolysis and beyond. *Lancet Neurol.* 2018;17(12):1121-1132.

65. Rajan WD, Wojtas B, Gielniewski B, et al. Defining molecular identity and fates of CNS-border associated macrophages after ischemic stroke in rodents and humans. *Neurobiol Dis.* 2020;137:104722.

66. Pedragosa J, Salas-Perdomo A, Gallizioli M, et al. CNS-border associated macrophages respond to acute ischemic stroke attracting granulocytes and promoting vascular leakage. *Acta Neuropathol Commun.* 2018;6(1):76.

67. Kumari R, Sinha K. Neutrophil in diabetic stroke: emerging therapeutic strategies. *Neural Regen Res.* 2021;16(11):2206-2208.

68. Wanrooy BJ, Wen SW, Wong CH. Dynamic roles of neutrophils in post-stroke neuroinflammation. *Immunol Cell Biol.* 2021;99(9):924-935.

69. Chen R, Zhang X, Gu L, et al. New insight into neutrophils: a potential therapeutic target for cerebral ischemia. *Front Immunol.* 2021;12:692061.

70. Candelario-Jalil E, Dijkhuizen RM, Magnus T. Neuroinflammation, stroke, blood-brain barrier dysfunction, and imaging modalities. *Stroke.* 2022;53(5):1473-1486.

71. Qiu Y, Zhang C, Chen A, et al. Immune cells in the BBB disruption after acute ischemic stroke: targets for immune therapy? *Front Immunol.* 2021;12:678744.

72. Drieu A, Lanquetin A, Levard D, et al. Alcohol exposure-induced neurovascular inflammatory priming impacts ischemic stroke and is linked with brain perivascular macrophages. *JCI Insight.* 2020;5(4):e129226.

73. Louet ER, Glavan M, Orset C, Parcq J, Hanley DF, Vivien D. tPA-NMDAR signaling blockade reduces the incidence of intracerebral aneurysms. *Transl Stroke Res.* 2022;13(6):1005-1016.

74. Hu K, Yang J, Tanaka S, Gonias SL, Mars WM, Liu Y. Tissue-type plasminogen activator acts as a cytokine that triggers intracellular signal transduction and induces matrix metalloproteinase-9 gene expression. *J Biol Chem.* 2006;281(4):2120-2127.

75. Kolb H. Mouse models of insulin dependent diabetes: low-dose streptozocin-induced diabetes and nonobese diabetic (NOD) mice. *Diabetes Metab Rev.* 1987;3(3):751-778.

76. Weide LG, Lacy PE. Low-dose streptozocin-induced autoimmune diabetes in islet transplantation model. *Diabetes.* 1991;40(9):1157-1162.

77. López-Atalaya JP, Roussel BD, Ali C, et al. Recombinant Desmodus rotundus salivary plasminogen activator crosses the blood–brain barrier through a low-density lipoprotein receptor-related protein-dependent mechanism without exerting neurotoxic effects. *Stroke.* 2007;38(3):1036-1043.